

# The volcanic debris avalanche on the SE submarine slope of Nisyros volcano, Greece: geophysical exploration and implications for subaerial eruption history

Isidoros Livanos · Paraskevi Nomikou ·  
Dimitris Papanikolaou · Grigoris Rousakis

Received: 12 January 2013 / Accepted: 25 July 2013 / Published online: 16 August 2013  
© Springer-Verlag Berlin Heidelberg 2013

**Abstract** A spectacular hummocky topography was discovered offshore of the south-eastern slope of the Nisyros island volcano in the eastern sector of the Aegean volcanic arc in 2000–2001, using multibeam bathymetric mapping and seismic profiling, and interpreted as part of a volcanic debris avalanche originating onland. During E/V *Nautilus* cruise NA011 in 2010, a detailed side-scan sonar and ROV exploration aimed at evaluating the surface morphology of this avalanche field. Combining the new data with selected older datasets reveals that the debris avalanche is characterized by numerous (at least 78) variously sized and shaped hummocks. Some of these are distinctly round, either scattered or aligned in groups, whereas others are elongated in the form of ridges. This is consistent with existing models accounting for variations in the longitudinal and lateral velocity ratio of landslides. Maximum dimensions reach 60 m in height above the sea bottom, 220 m in length and 230 m in width. The structures outline a large tongue-shaped, submarine hummock field of about 22.2 km<sup>2</sup>, approx. 4.8 km wide and 4.6 km long and with an estimated volume of 0.277 km<sup>3</sup>. Due to its characteristic shape, the collapsed volcanic flank is interpreted to represent a singular failing event, involving a rapid and virtually instantaneous downslope movement of the slide mass into the sea. Indeed, the H/L (height of 280 m vs. run-out of 7 km) ratio for the Nisyros slide is 0.04; plotted against volume, this falls within the theoretical bounds as well as measured values typical of submarine landslides. The timing of the event is probably related to the extrusion of Nikia lavas and their subsequent failure and formation of a main scarp observed at

about 120 m depth on an 8-km-long seismic profile and a map of slope angle distribution, at the depth where the palaeo-coastline was located 40 ka ago. An inferred age of ca. 40 ka for the avalanche awaits confirmation based on dating of core material.

## Introduction

Large submarine volcanic debris avalanches associated either with an edifice collapse or with large-scale destabilizations and collapse of the flanks of volcanic edifices are among the most catastrophic and hazardous events on earth. The volumes of the resulting deposits can reach several cubic kilometres and, because of their rapid downslope movement, can threaten whole populations and infrastructures. Such avalanches can travel up to 100 km away from the source, the process beginning with a large-scale rock or sediment slide that rapidly transforms into a fast-moving debris avalanche with increasing travel distance (e.g. Voight et al. 1983; Glicken 1991). Although not necessarily triggered by volcanic eruptions, debris avalanches accompany the evolution of most volcanoes, particularly stratovolcanoes such as the island of Nisyros in the Aegean Sea, Greece, and thereby effectively limit the vertical growth of volcanoes (Carey and Schneider 2011). Among all volcanic debris avalanches (VDAs) recognized on earth, submarine VDAs are the most voluminous and most mobile, the effective friction coefficients lying in the range of  $0.03 < H/L < 0.13$  (Shaller 1991).

The deposits of flank collapses commonly form characteristically horseshoe-shaped depressions (e.g. Voight et al. 1981). Modern oceanographic survey techniques involving high-resolution swath bathymetry, side-scan sonar and ROV (remotely operated vehicle) exploration greatly facilitate the recognition of their typical hummocky topography. Remnant scarps from collapse events can be found in both subaerial and submarine environments (e.g. Lipman et al. 1988). Classical

I. Livanos · P. Nomikou (✉) · D. Papanikolaou  
Department of Geology and Geoenvironment, Panepistimioupoli  
Zografou, University of Athens, 15784 Athens, Greece  
e-mail: evinom@geol.uoa.gr

G. Rousakis  
Hellenic Centre for Marine Research, Institute of Oceanography,  
P.O. Box 712, 19013 Anavyssos, Attiki, Greece

examples are known from the Lesser Antilles arc in the Caribbean Sea, where more than 52 debris avalanche deposits have been identified on the seabed (Deplus et al. 2001), the Canary Islands, where giant landslides are associated with hummocky topography forming horse-shoe shaped structures (Krastel et al. 2001), and the Hawaiian Islands where the Alika debris avalanche (volume of about 2,000 km<sup>3</sup>) is one of the largest documented so far (Lipman et al. 1988). In the Aegean Sea, submarine VDAs have been found more recently in the vicinity of several volcanic islands, including Antimilos (Alexandri et al. 2001; Nomikou et al. 2013), Santorini (Bell et al. 2013) and Nisyros (Tibaldi et al. 2008; Nomikou et al. 2009). Indeed, the utility of nearshore geophysical exploration in gauging the past, present and future evolution of volcanic islands is currently experiencing an upsurge in interest worldwide—e.g. the Azores (Mitchell et al. 2012), the West Indies (Cassidy et al. 2013) and the Canary Islands (Fontán Bouzas et al. 2013).

In the eastern sector of the Aegean volcanic arc in the Aegean Sea, Tibaldi et al. (2008) and Nomikou et al. (2009) reported the discovery of a spectacular field of hummocky topography offshore of the south-eastern slope of the Nisyros island volcano. Combining onland data with nearshore multibeam bathymetric mapping and seismic profiling, this was interpreted as part of a debris avalanche that originated onshore where it involved the Nikia lava flows. Along their flanks, these lava fields are bounded by three distinct scarps, two of which are located in the southwest and one in the northeast. The offshore data revealed numerous round and elongated hummocks (ridges) of heights reaching 60 m, covering a horseshoe-shaped area (in plan view) of about 16 km<sup>2</sup> with an average thickness of 40–50 m at water depths of 250–380 m.

In the present article, the surface morphology and subsurface structure of this submarine hummock field are explored in greater detail, by combining older bathymetric and seismic datasets with newer information obtained by side-scan sonar and ROV surveys. In an attempt at verifying the nature of the debris avalanche, the findings are evaluated in terms of key criteria typifying landslides, notably existing models of longitudinal and lateral velocity ratios, and height/run-out/volume interrelations. Finally, possible triggering mechanisms and the age of the landslide event are discussed.

### Physical setting

The Hellenic volcanic arc has developed in the back-arc region of the Hellenic subduction zone (Fig. 1), parallel to and about 150 km north of the Peloponnese–Crete–Rhodos island arc (McKenzie 1970; Le Pichon and Angelier 1979). It is the result of at least 45 Ma of subduction of the East Mediterranean oceanic lithosphere below the European continental plate (Papanikolaou 1993). The geodynamic structure

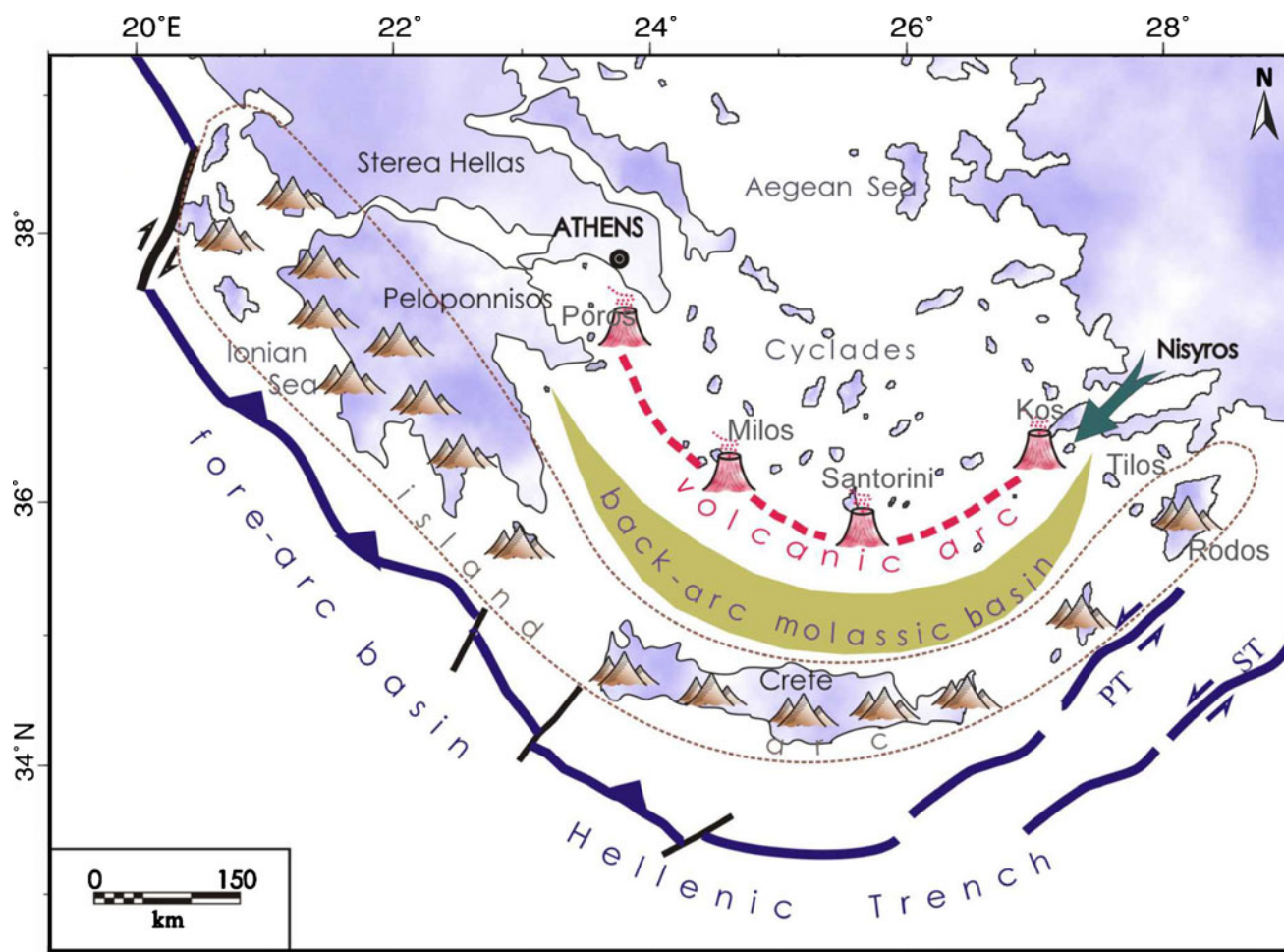
of the Aegean arc includes the Hellenic Trench, which is a 1,500-km-long arcuate series of troughs located south of Crete extending from the Ionian Sea in western Greece to the Libyan Sea, and terminating southeast of the island of Rhodos. It also includes the island arc comprising the Peloponnese, Crete and the Dodekanese Archipelago, and the back-arc mollassic basin of the Cretan Sea. The Hellenic volcanic arc has developed parallel to and behind the island arc. Recent active volcanoes occur on Soussaki, Methana, Aegina and Poros in the west, on Milos and Santorini in the centre, and on Kos and Nisyros in the east. Besides these onshore volcanoes, several submarine volcanoes have been discovered over past decades in the course of marine geophysical surveys (for overview, see Nomikou et al. 2013).

The volcanic island of Nisyros is located between the islands of Kos and Tilos in the south-eastern Aegean Sea (Fig. 1). It has a spectacular relief characterized by a truncated volcanic cone with a base diameter of 8 km and a caldera in the middle of the island 4 km in diameter. It is composed of mostly Quaternary volcanic rocks represented by alternating lava flows, pyroclastic layers and viscous lava domes, ranging in age from 200 to 25 ka (Papanikolaou et al. 1991). The only historical reports of hydrothermal eruptions are from 1871–1873 and 1887 AD, these having been accompanied by violent earthquakes, gas detonations, steam blasts and mudflows (Marini et al. 1993).

### Materials and methods

In 2000–2001, 2009 and 2010, geophysical exploration offshore of Nisyros involved deployment of (1) a swath bathymetric SEABEAM 2120 system for deep (>500 m) and a SEABEAM 1180 system for shallow waters (<500 m), (2) an EdgeTech 4200 MP 300/600 kHz side-scan sonar, (3) Hercules and Argus ROVs, (4) a Datasonics sparker seismic profiling system with a 2,000 J SIG 2mille sparker energy source, allowing subbottom penetration depths of up to 1,000 m in water depths up to 1,500 m, and (5) a hydrophone array, receiver and digital recording system of S.I.G. The multibeam bathymetric survey was carried out from aboard the R/V *Aegaeo* of the Hellenic Centre for Marine Research (HCMR) during three successive cruises conducted in 2000 in the region of the Nisyros–Kos islands, as part of the GEOWARN scientific program.

During E/V *Nautilus* cruise NA011 in October 2010, detailed side-scan sonar and ROV surveys were carried out within the framework of the New Frontiers in Ocean Exploration 2010 collaborative project. Hercules and Argus ROVs are state-of-the-art deep-sea robotic vehicle systems capable of operating at depths up to 4,000 m. Both vehicles are equipped with high-definition (HD) video cameras and 1,200 W lamps. Hercules also has two manipulator arms. For



**Fig. 1** Simplified regional map showing the modern Hellenic volcanic arc north of the Hellenic Trench, the Peloponnese–Crete–Rhodos island arc and the Cretan back-arc basin (extracted from Nomikou and Papanikolaou 2011)

the purpose of the high-resolution side-scan survey, Argus was fitted with an EdgeTech sonar system (see above).

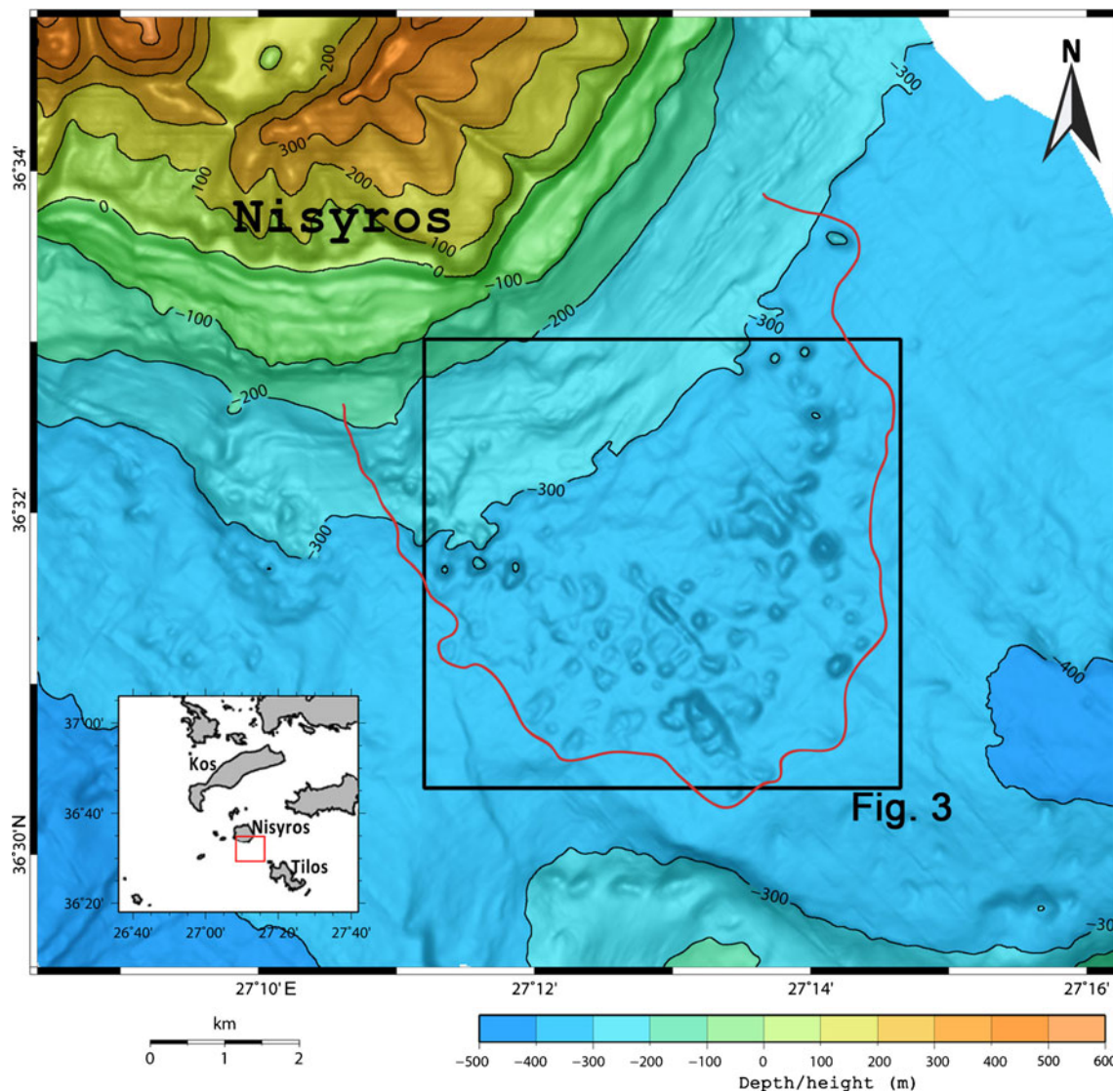
**Results**

The detailed bathymetric data were compiled into a swath bathymetric map of the study area at a scale of 1:40,000 (Fig. 2), the 11 different colours defining the onshore/offshore relief at 100 m elevation/isobath intervals. The bathymetry SE of Nisyros shows numerous round and elongated hummocks extending from the southern to the south-eastern slopes of the island. The heights of these features above the surrounding seabed range from several metres to 60 m in some cases. The density distribution of hummocks changes with distance from the shore. Some are in contact with each other, while others form elongated ridges aligned in a NW–SE direction. Together they define a tongue-shaped field with most hummocks concentrated at the periphery at water depths of 250 to 370 m. More than 50 hummocks were identified on

the bathymetric map, whereby areas of scattered hummocks can be distinguished from areas of aligned hummocks (Fig. 3).

On the basis of the bathymetry, a slope angle map showing five pooled slope intervals was generated (Fig. 4a): (1) sub-horizontal areas with mean slopes of 0–3°, (2) low slope areas of 3–6°, (3) moderate slope areas of 6–10°, (4) steep slope areas of 10–20° and (5) very steep slope areas greater than 20°. Low slope areas (up to 3° slope angles) define flat areas where the seafloor is relatively smooth without marked morphological differentiation. Moderate slopes define circular areas occupied by hummocks. Steep and very steep slope areas, by contrast, are associated with tectonic fault zones, linear volcanic zones or avalanche deposits. Of these, the avalanche deposits are defined by slope areas ranging from 3–20°, whereas very steep slope values correspond to the linear marginal fault zone of the Tilos Basin in the southern part of the region and the SE coastal zone of Nisyros where very steep slopes exceeding 20°, as well as intermediate linear zones with slopes up to 20° are orientated NE–SW.

Two prominent linear features with steep slopes are of particular interest. They are located in the centre of the horseshoe-



**Fig. 2** Bathymetric map from multibeam data with 20 m cell resolution, showing the boundaries of the tongue-shaped hummock field SE of Nisyros

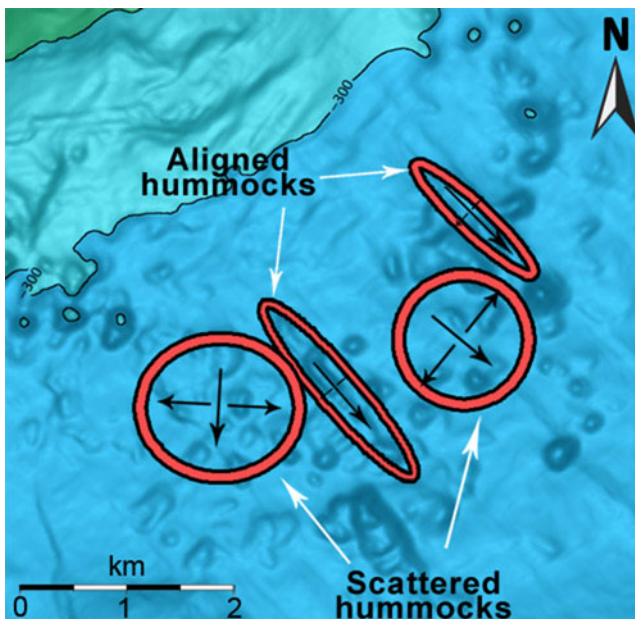
shaped hummock field, where they stand out from other steep features. These linear structures occur at approx. 250 m water depth. The slope vs. depth profile (Fig. 4b) shows that the central internal area has a smooth surface, whereas the rough seafloor over the hummock field has gradients up to 20°.

Focusing on the debris avalanche area, the azimuths of seafloor fabric orientations (11,258 values) were determined and plotted into a rose diagram incorporating all slope categories (Fig. 5a). From the rose diagram it is evident that the main directions of the seafloor fabric are aligned S–SE, which is also the main direction of the debris avalanche. This is also obvious from the 3D digital terrain model of Fig. 5b, which clearly highlights the tongue shape of the hummocky area indicating the flow direction of the debris avalanche.

Using generic mapping tools, the area and volume of the deposit were calculated from the bathymetric data (Fig. 6). The deposit volume corresponds to the difference between ‘before’

and ‘after’ grids. The latter grid represents the present-day topography extracted from the multibeam bathymetry (upper left of Fig. 6), whereas the former grid (lower left of Fig. 6) was generated by applying the polygon method to mask out the deposit from the multibeam data (upper right of Fig. 6). It is demonstrated that the offshore debris avalanche field on the SE flank of Nisyros volcano covers ~22.2 km<sup>2</sup> with a volume of 0.277 km<sup>3</sup>.

The side-scan sonar mosaic reveals an even more complex physiography than does the bathymetry on its own. A total area of approx. 26.5 km<sup>2</sup>, covering roughly 80 % of the hummocky area, was surveyed with the 300 kHz side-scan sonar. The side-scan mosaic (Fig. 7) reveals 78 hummocks in all. Moreover, there is a high abundance of hummocks south of the central sector, associated with disturbed sediment deposits. This emphasizes the value of additional detailed mapping by side-scan sonar. In general, the central part of the side-scanned area is very rough



**Fig. 3** Zoomed area of the bathymetric map of Fig. 2, showing examples of aligned and scattered hummocks

and also displays the largest hummocks, some attaining heights of more than 25 m. The seafloor at the edges of the debris avalanche (left and upper right of the centre in Fig. 7) is smoother but still displays large hummocks. A closer look at these shows them to be flat-topped with vertical sides, many occurring in clusters concentrated mainly in the lower centre of the avalanche area.

Descriptive statistics and analysis of the raw side-scan data and the processed mosaic tend to provide more information for the hummocky area. Several characteristics (length, width, height and area) were measured and/or calculated for each of the 78 individual hummocks, and selected datasets then plotted against the run-out distance from the Nisyros shore. The shoreline of Nisyros (water depth of 0 m) was used as the vertical reference point. The results show that hummock abundance is quite variable at distances between 2 and 7 km from the shore, the maximum number being concentrated within the 4–5.5 km range (Fig. 8). The lengths of the hummocks range from 19–220 m (measured along-track), whereas widths range from 16–236 m. Hummock areas and heights also vary significantly, the former ranging from 366–51,965 m<sup>2</sup>, the latter from 3.5–30.7 m. These measurements correspond to volumes of 1,737–1,115,684 m<sup>3</sup>. Average hummock heights centre around 12 m (calculated from the shadow lengths visible on the side-scan records).

Analyzing four seismic profiles crossing the debris avalanche area, it was possible to identify four different seismic units on the basis of their internal structure and stratigraphic position (Fig. 9), the labels starting with A for the youngest (top) package and ending with C for the oldest one. A seismic profile showing most of the important features is AK18-5D

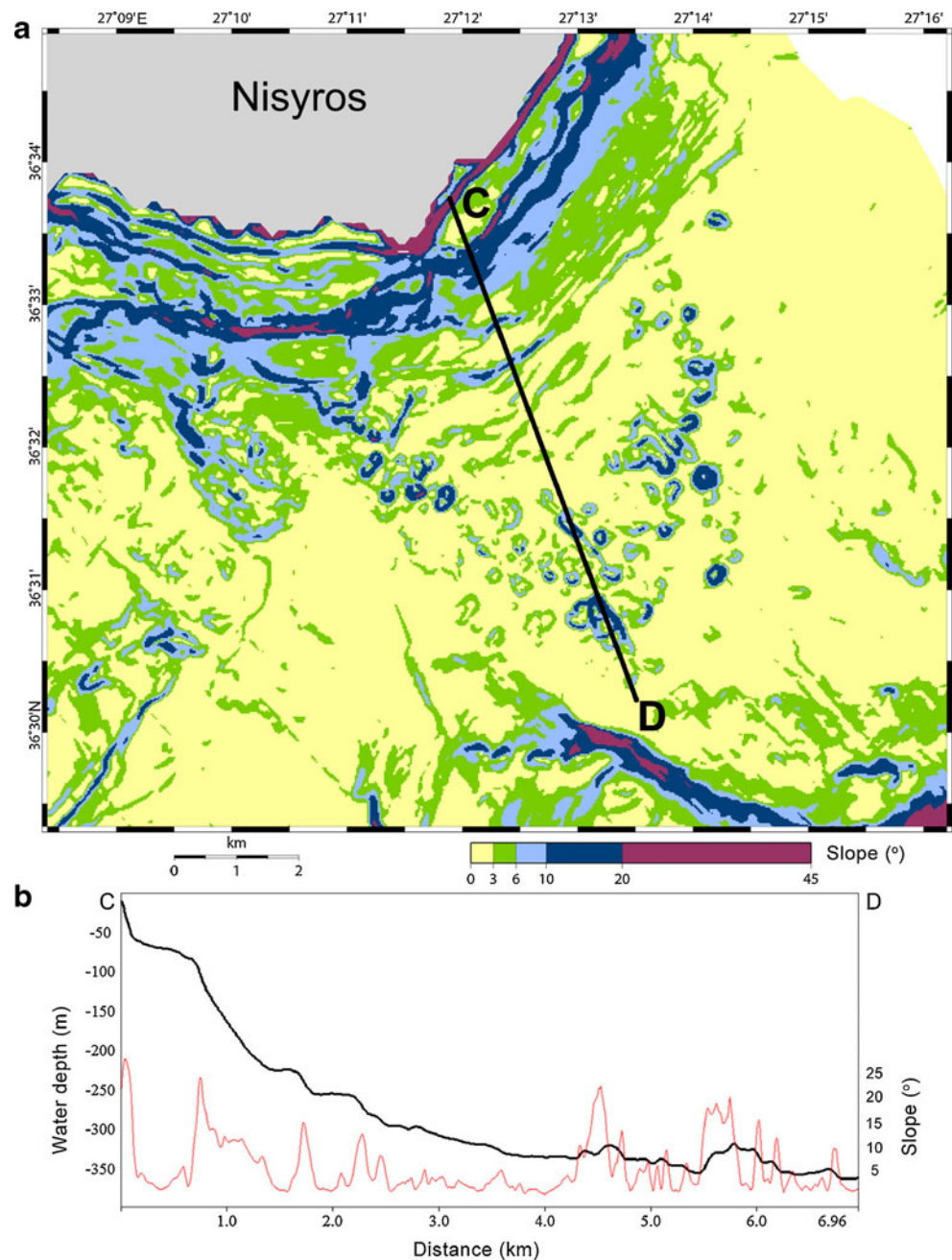
(Fig. 10), which runs S–N starting at 310 m water depth north of Tilos island and heads northwards towards Nisyros island. Approximately 6 km long, this profile crosses the western part of the debris avalanche deposits and ends on the Nisyros island slope at 200 m water depth.

Starting in the south, two seismic units can initially be identified. An uppermost one, labelled A1 on Fig. 10, represents late Pleistocene and Holocene sediments. This is underlain by a seismic sequence labelled unit C on Fig. 10, which is occasionally dissected by columnar seismic blanking structures overlain by pull-up reflectors creating a chimney-like signature. The profile then crosses the tectonic boundary fault zone of Tilos, the vertical offset showing that the island has been uplifted (Tilos horst). Moving northwards, seismic units A1, A2, B and C are interrupted by a number of hummocks displaying hyperbolic reflectors produced by the steep topography. The largest hummock peaks at 15 m above the seabed and is topped by a sediment cover. The slope ascending towards Nisyros is characterized by a step-like morphology, including a rotational slump; the steps are separated by slide scarps, documenting that a large section of the seafloor slid downslope towards the south. North of the hummocky area, only late Pleistocene sediments occur, being represented by units A1 and A2. These directly overlie the volcanic basement.

Seismic profile AK18A (Fig. 11) runs N–S, starting SE of Nisyros volcano from where it crosses the central part of the submarine debris avalanche and ends north of Tilos. It is approx. 8 km long. The profile starts at a water depth of 290 m and progresses southwards into deeper water, reaching a maximum depth of 350 m before ascending the steep slope towards Tilos. Along the first section of the profile (left side of Fig. 11), the acoustic stratigraphy reveals seismic unit A1, which forms the uppermost sediment layer and reaches a maximum thickness of 5.7 m. It is underlain by seismic unit A2, which is occasionally only faintly visible. The parallel reflectors of seismic unit A1 follow the undulating seafloor morphology, the lowermost bed sometimes toplapping sub-adjacent units. Below the bottom layer of unit A1, the resolution of the seismic profile is unfortunately too poor to enable the detection of a listric plane that would indicate a glide plane or any deformation before deposition of the A1 sediment sequence. However, the morphology and overall attitude of unit A1 suggests that the late Pleistocene marine sediments were deposited on a wavy seafloor that was possibly deformed by tectonic processes.

Moving southwards towards the middle section of the profile, a complex hummocky topography bounded by hyperbolic reflectors is encountered. The hummocks are clearly seen to be topped by parallel-bedded sediment, any reflectors that may be present beneath the structures being (as in the case of Fig. 10) masked by the hyperbolic signatures. The hummocky topography represents the Nisyros debris avalanche deposit. Towards Tilos the seabed becomes smoother and the

**Fig. 4** **a** Slope distribution map of the study area. **b** Depth and slope profiles crossing the avalanche deposit along the NW–SE transect (c–d) shown in **a**

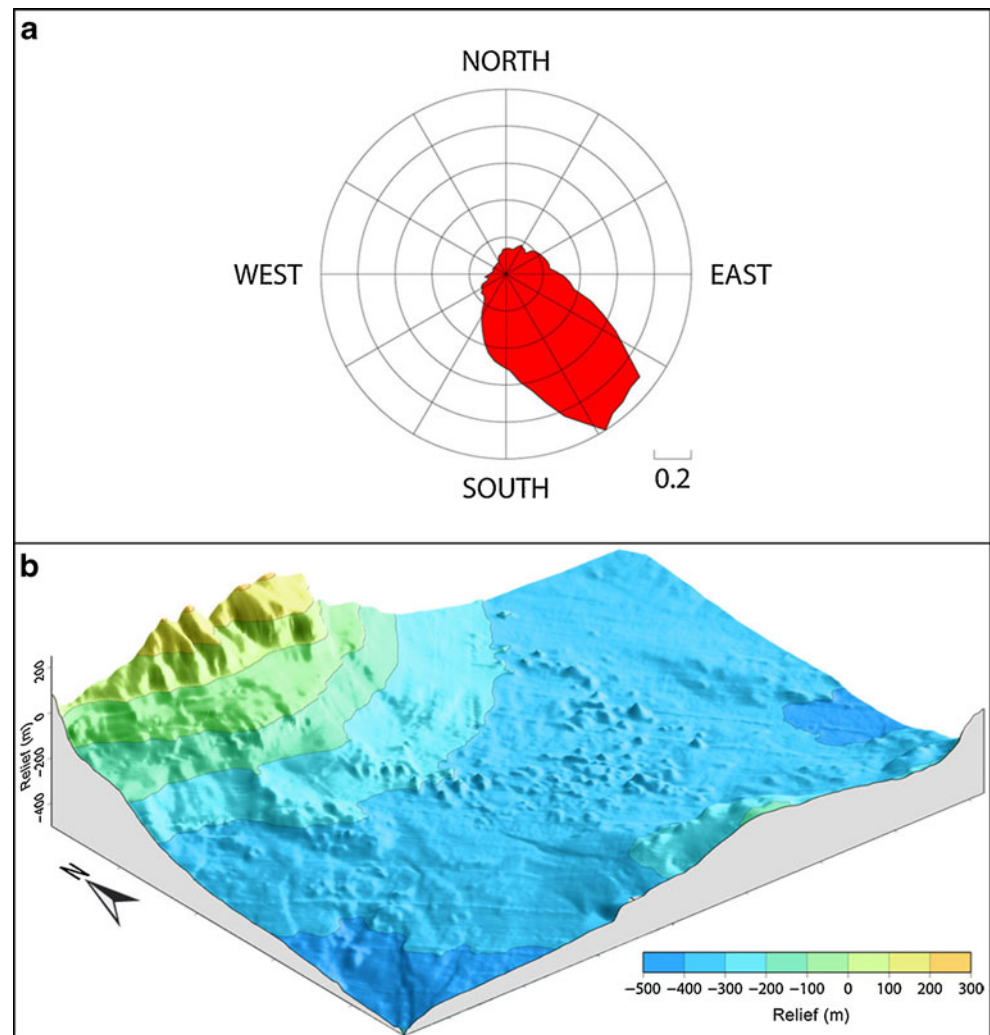


acoustic stratigraphy more clearly visible, showing the presence of four vertically stacked seismic units. The uppermost sediment sequence can again be subdivided into the two seismic units A1 and A2 (Fig. 9). In this part of the profile, unit A1 is thicker than north of the hummocky area, reaching a maximum thickness of 12 m. Unit A2 following below unit A1 has a maximum thickness of 5 m. Whereas both upper units are parallel-bedded, the unit underlying A2 (seismic unit B) is characterized by chaotic internal reflectors with a

maximum thickness of 16.5 m. Another parallel-bedded sedimentary sequence (unit C), located between seismic unit B and the acoustic basement, reaches a maximum thickness of 16 m along this profile.

Southwards, the latter parallel-bedded sequence is truncated by the Tilos tectonic boundary fault zone, which separates the Tilos tectonic horst from the Nisyros volcanic field to the north (Nomikou and Papanikolaou 2011). It has a vertical throw of more than 1.4 km, thereby exposing the alpine

**Fig. 5** **a** Azimuth orientations of seafloor fabric in the debris avalanche area. **b** Three-dimensional terrain model of the larger study area (cf. Fig. 2)



basement and post-Alpine sediments at the southern end of profile AK18A. Seismic units B and C have a S–N orientation, thinning towards Tilos and tending to thicken northwards. The two units were probably part of the Tilos basin deposits before being disrupted by the eruption of the Nisyros volcano.

The ROV exploration in 2010, with the deployment of an Argus-mounted HD camera from aboard E/V *Nautilus*, lasted 3 h and served for a closer visual inspection of the hummocks outcropping at the avalanche site. Of the 78 hummocks identified on the side-scan mosaic, six were targeted in the eastern sector (cf. Fig. 7). All were found to be covered with biological encrustations, rendering the visual identification of the outcrop material difficult, if not impossible. In some cases, black-coloured patches on round hummocks (22 m high, Fig. 12a) suggest the presence of volcanic rock possibly originating from shallow water near the coastline. Another target (23 m high, Fig. 12b) oriented at  $108^\circ$  has a gentle

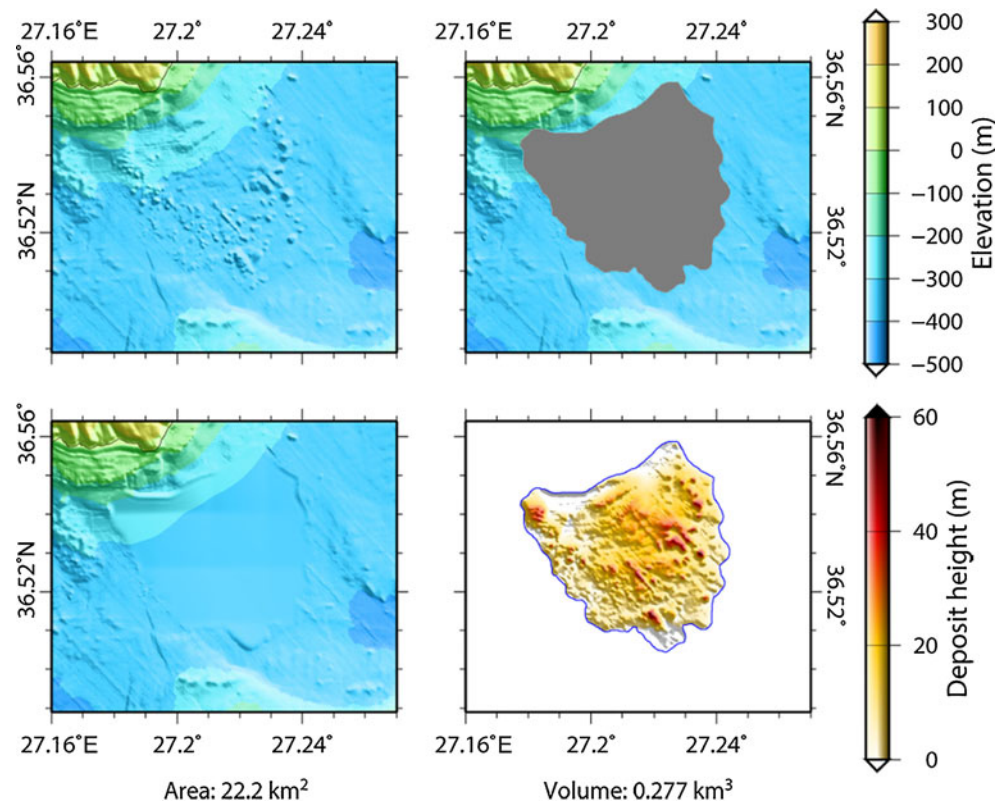
northern slope and a steeper southern one, the asymmetrical shape having perhaps been produced by compression that resulted in the formation of a NE–SW-oriented ridge.

### Discussion and conclusions

#### Morphology and dimensions of submarine hummock field

Tibaldi et al. (2008) suggested that the hummock field covers an area of approx.  $16 \text{ km}^2$  at water depths of 250–380 m. The new data show that the field actually extends over approx.  $22.2 \text{ km}^2$ —which exceeds the former estimate by 26 %—at a somewhat wider range of water depths from 230–380 m. It comprises at least 78 hummocks of less than a metre to nearly 230 m in length and width, covering an area approx. 4.8 km wide by 4.6 km long. The tongue shape of the hummock field suggests a south-easterly ( $150^\circ$  azimuth) flow direction of the

**Fig. 6** Volume and area calculations of the avalanche deposit. *Upper left* Present-day topography, *lower left* pre-landslide topography, *upper right* landslide area polygon, *lower right* total deposit volume



avalanche. The main concentration of hummocks occurs in the peripheral area of the field, the structures having vertical sides and occasionally flat tops, and ranging in height from 8–18 m. The offshore volume of this debris deposit is here estimated to be about 0.277 km<sup>3</sup>, the total volume of the collapse from the summit of Nisyros volcano having been estimated at 1 km<sup>3</sup> by Tibaldi et al. (2008).

Two types of areas were identified, one displaying scattered hummocks, the other aligned hummocks (Fig. 3). Considering the morphology of the seafloor when the avalanche came to rest, and following the model proposed by Dufresne and Davies (2009), the mode of deposition reveals the lateral velocity structure as a function of distance from the centre of the flow. The avalanche material moves fastest along the central, longitudinal flow path, the speed progressively decreasing laterally away from the centre. Along the fast track, longitudinal ridge and flowband formation is favoured. Laterally, where the flow speed is slightly less, hummocks and ridges tend to break up into clusters (Dufresne and Davies 2009) to form aligned hummocks. This is especially the case in the decelerating distal parts of many rock and debris avalanches where the flow spreads out laterally.

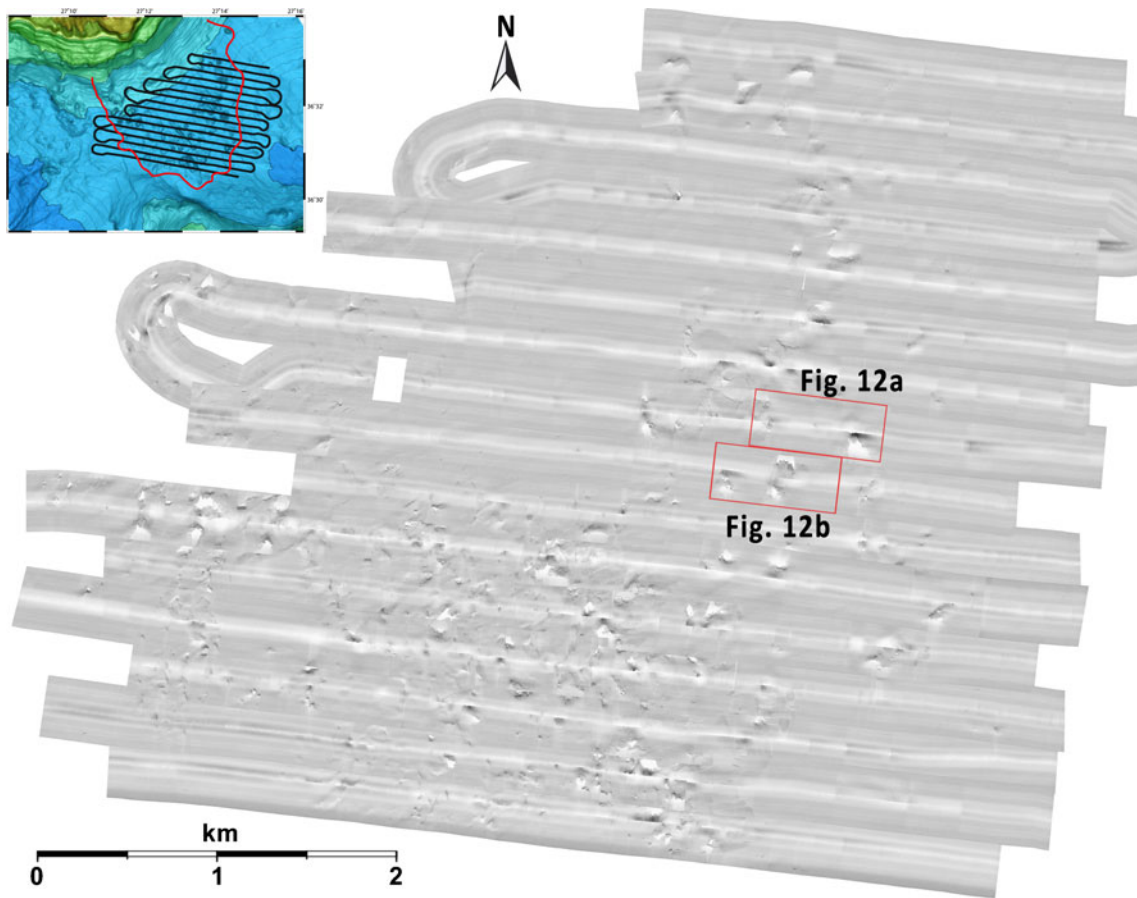
Analyzing the slope distribution of the study area, the low-angle areas defined by yellow (0–3°) and green (3–6°) colours in Fig. 4a are located mainly in the basin and in the

semicircular zone upslope of the hummocky area. Steep slopes (blue and red colours) exceeding 10° are observed close to Nisyros island, where they form scarps occupying specific depth intervals probably created by subaerial erosion during Pleistocene sea-level lowstands, and near the island of Tilos where they define an E-W-oriented major fault zone. Besides these two obvious regions, steep slopes are also observed around many hummocks, especially to the SE of Nisyros where they trace the tongue-shaped hummock field formed by the debris-flow deposit.

#### Seismic stratigraphy

Analysis of the sparker seismic reflection profiles reveals that the Nisyros debris avalanche deposit forms the youngest seismostratigraphic unit southeast of the island, its chaotic and occasionally hyperbolic nature being in agreement with this kind of deposit. The hyperbolic reflectors mostly mask seismic return signals from beneath. However, localized evidence for the presence of horizontal reflectors below these structures preclude them to be basement protrusions (Fig. 10), and therefore imply these to be associated with the debris avalanche deposit. The columnar acoustic blankings topped by pull-up structure reflectors observed in the stratified sediment layers of unit C (Fig. 10) may have resulted from the disruption of sediment strata by the upward migration of gases and/or pore fluid, a signature documented in numerous settings worldwide (Løseth et al. 2009).





**Fig. 7** Side scan mosaic of the Nisyros debris avalanche. Upper left map shows sidescan sonar transects combined with the swath bathymetry. The red line indicates the boundaries of the tongue-shaped hummock field SE of Nisyros

These blanking zones are observed on the southern tectonic block immediately adjacent to the Tilos marginal fault, with which they may be associated.

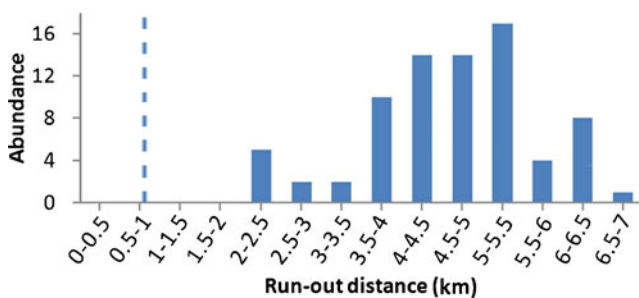
Scars and slip plane geometries

Identification of slide scars and glide planes enables a comparison of the failed slope segment with nearby non-failed areas. The information gained from this can be useful in uncovering the reasons for failure (Canals et al. 2004). In the present case, two linear features were identified (Fig. 4a) in the

middle sector of the back-arc of the avalanche deposit, characterized by steep slopes. These linear features are confidently interpreted as slide scars because of their shape, their position relative to the deposit and their location along seismic profile AK18-5D (Fig. 10). The occurrence of two secondary scarps with back tilting at 250 m depth does not exclude the possibility of other slide scars existing higher on the flank. The well-defined bathymetric zone around 100 m water depth, characterized by slopes of 10–45°, forms the main scarp of the landslide (Fig. 4a).

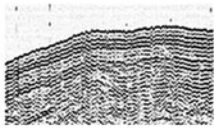
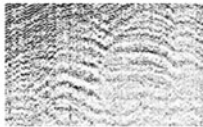

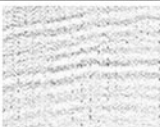

Run-out distance

Run-out is the horizontal distance from the upper edge to the farthest point of the slide mass. Based on the available data for the Nisyros hummock field, the run-out of most avalanche sections was less than 5 km from the assumed source, some reaching 7 km. Comparing the total change in height with the total run-out (H/L) gives an indication of the overall mobility of a slide, although it would not account for transitions between different stages of a mass movement event, as in the case of a slump that transforms into a debris avalanche.



**Fig. 8** Hummock abundance vs. run-out distance from shore. Dashed line Approximate start position of the landslide

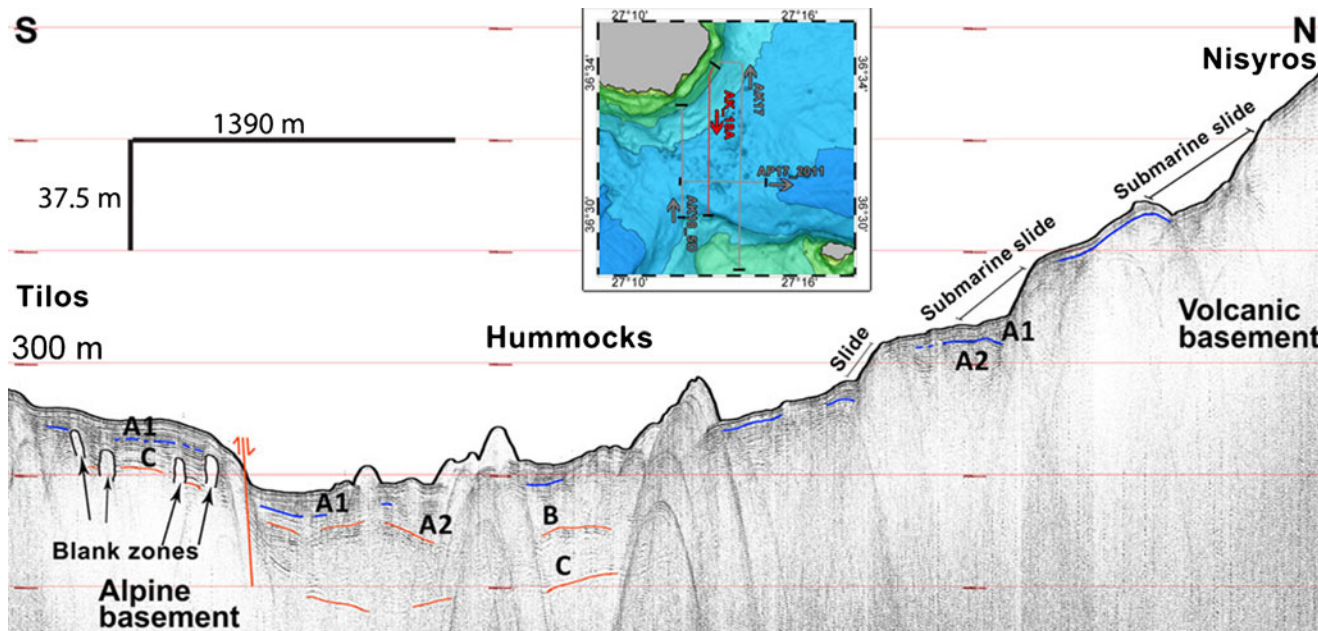
**Fig. 9** Characteristics of seismic units identified in two N–S seismic profiles across the study area (see Figs. 10 and 11)

| Acoustic unit                | Reflection characteristics   | Type example  |
|------------------------------|--|---|
| <b>A1</b>                    | Characterized by parallel reflection configurations. The lower boundary toplaps sub-adjacent units. The reflectors are low amplitude and high frequency. Maximum layer thickness recorded – 13.5 m   |  |
| <b>A2</b>                    | Characterized by a wavy reflection configuration. Reflector amplitudes range from moderate to high, are largely continuous and frequency tends to be uniform. Maximum layer thickness recorded -14 m. The upper boundary displays erosional truncation |  |
| <b>B</b>                     | Characterized by chaotic internal reflectors. Maximum layer thickness recorded – 18 m  |  |
| <b>C</b>                     | Characterized by a parallel and at times sub-parallel reflection configuration. The reflectors are high amplitude, continuous and frequency tends to be uniform. Maximum thickness recorded – 28 m   |  |
| <b>Hyperbolic reflectors</b> | Acoustically transparent reflectors with hyperbolic reflections on the upper boundary  |  |

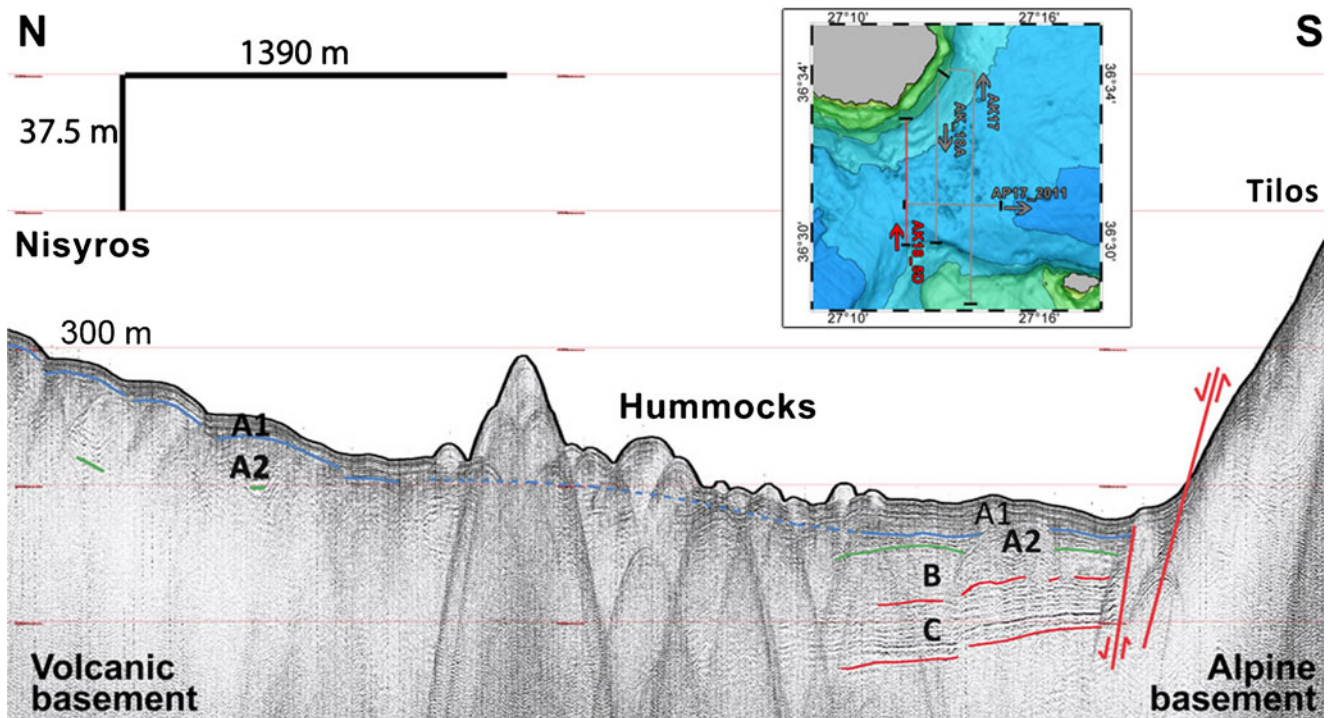
Typical values for underwater landslides range from  $10^{-3}$  to  $10^0$ , smaller values indicating higher mobility (Siebert 1984; Canals et al. 2004). The H/L for the Nisyros slide is 0.04 (using a run-out of 7 km); when plotted against volume, this falls not only within the theoretical bounds but also within the range of values typical of submarine landslides (Fig. 13).

Triggering mechanisms and dating

At a sedimentation rate of 21.8 cm/1,000 years (cf. below for independent data sources), the thickness of the sediments (almost 9 m) overlying the landslide indicates an age of about 40 ka, which places it close to the extrusion period of the Nikia lavas (Tomlinson et al. 2012). The Nikia rhyolites expose



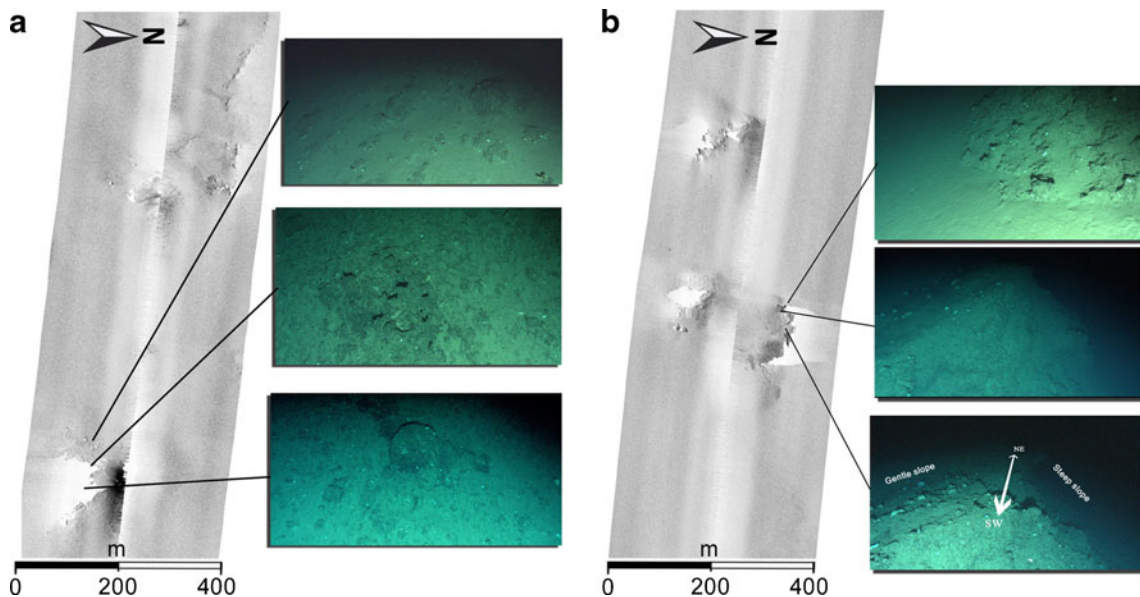
**Fig. 10** Seismic profile AK18-5D crosses the western part of the volcanic debris avalanche on the SE submarine slope of Nisyros volcano



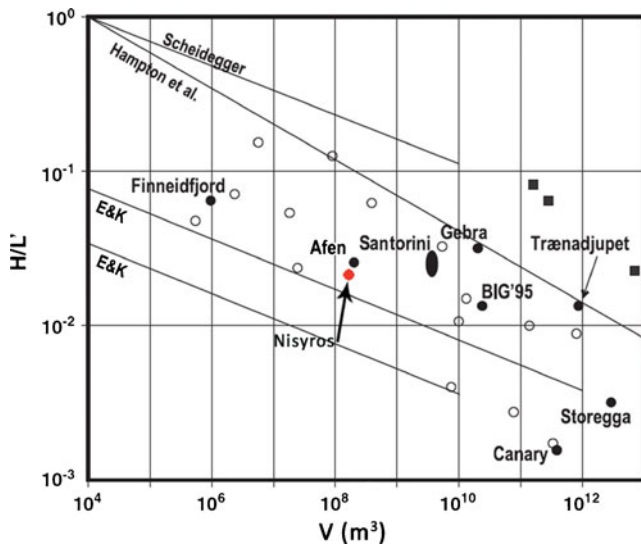
**Fig. 11** Seismic profile AK18A crosses the central part of the volcanic debris avalanche on the SE submarine slope of Nisyros volcano

impressive flow forms with folding and shearing along the SE coastline (Fig. 14, upper left). However, there is no major break in the onshore Nikia lava outcrops. On the contrary, at about 80–120 m water depth there is a well-defined 10–40 m high submarine scarp with a slope of 10–45° that runs sub-parallel to the coastline (Fig. 4b). This bathymetric zone corresponds to the palaeo-coast 40 ka ago (Lykousis 2009). Two secondary

minor scarps of 10–20 m height occur at 250 m depth (Fig. 4b). These exhibit a back-tilting geometry of the landslide material just above the basal slip surface (Fig. 14). The geometry of the SE area of Nisyros, both onshore and offshore, shows the contact zone of the Nikia lava with the underlying strato-volcanic structure, which probably represents the sliding surface, to be only a few metres thick.



**Fig. 12** ROV video observations (dive NA011) of selected hummocks identified in the side-scan sonar mosaic (for locations, see Fig. 7). **a** Target 23 and **b** target 24, both showing evidence of round black hummocks



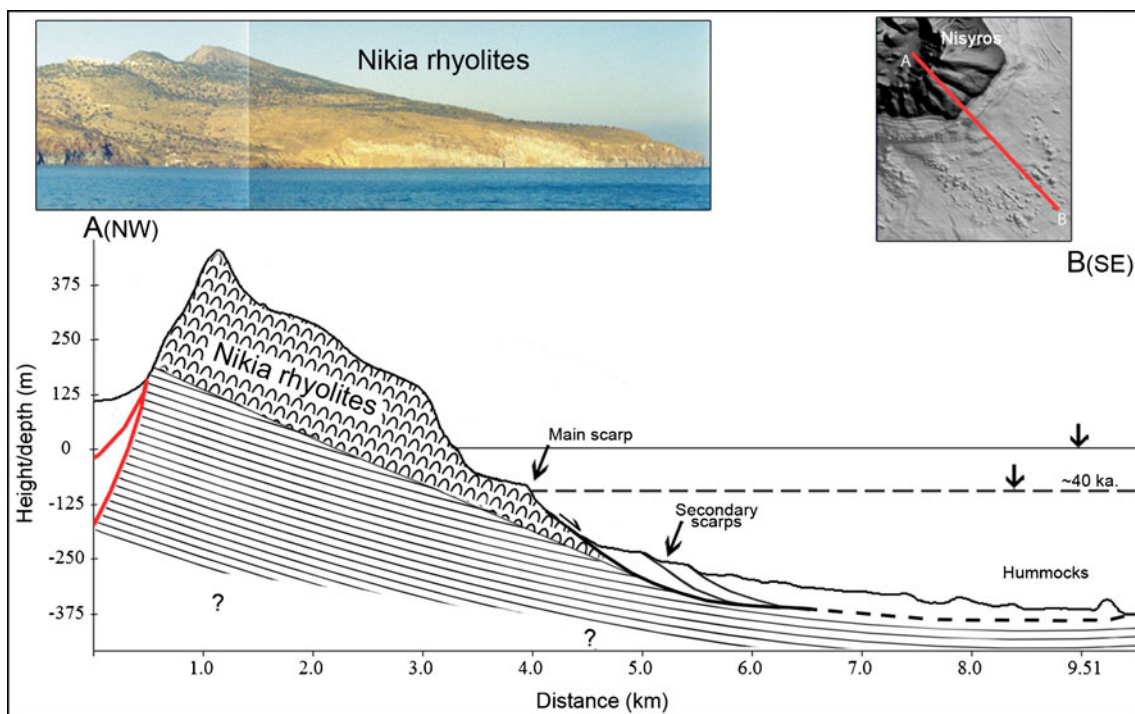
**Fig. 13** Mobility of submarine and subaerial landslides compiled by Canals et al. (2004, their Fig. 14), expanded by addition of the Nisyros (red circle, present study) and Santorini submarine landslides (Bell et al. 2013). For additional data sources, the reader is referred to Canals et al. (2004)

The most plausible scenario suggests the occurrence of a submarine landslide during or immediately after the Nikia lava flow, the 40 ka palaeo-coast at about 120 m depth probably playing a dominant role. The submarine landslide thus involved Nikia rhyolitic material and late Pleistocene

sediments flowing towards the SE across a smooth palaeo-surface dipping about 3° in the same direction.

There are no cores available from the debris avalanche area on which to perform dating. The ROV photos as well as the side-scan sonar and seismic profiles suggest that the greatest part of the debris avalanche deposit is covered by a thick layer of young Holocene sediments, implying an older age for the deformed sediments of the avalanche deposit. As a rough approximation, a sedimentation rate of 21.8 cm/1,000 years, calculated for the late glacial–Holocene in the western Kos Basin based on plankton/pollen data from Triantaphyllou et al. (2009a, 2009b) as well as geochemical data from Katsouras et al. (2010), is assumed. In combination with the observed depth of the erosional truncation of unit A2 (almost 9 m in the seismic profiles) plausibly induced by the avalanche, the timing of the event can be estimated at ~40 ka BP. This is consistent with the findings of Tibaldi et al. (2008), who suggested that the younger age limit of the collapse is 35 ka on the basis of Nikia lava datings.

In conclusion, the independent evidence presented above confirms the interpretation of Tibaldi et al. (2008) that an ancient massive SE flank collapse of the Nisyros volcano generated a debris avalanche that deposited material persisting up to the present day in an extensive hummock field close to the island. The inferred age of ca. 40 ka for the avalanche awaits confirmation by dating of core material.



**Fig. 14** Conceptual topographic section oriented NW–SE showing the well-defined main submarine scarp running sub-parallel to the coastline, the two minor scarps above the basal slip surface, and the sea level at ca. 40 ka BP (the latter based on Lykousis 2009)

**Acknowledgements** This work is a part of the GEOWARN project (contract no. IST-1999-12310). The European Commission is acknowledged for financial support. Additional funding was provided by the Institute for Exploration (IFE-USA) within the framework of the cooperative research project “New Frontiers in the Ocean Exploration 2010”. The officers and the crew of the R/V *Aegaeo* and E/V *Nautilus* are gratefully acknowledged for their important and effective contribution to the field work and sampling. K.L.C. Bell is thanked for operational support and participation in data collection. Vasilis Anagnostopoulos and George Anastasakis are thanked for sharing seismic profiles. Vasilis Lykousis, Alessandro Tibaldi, an anonymous reviewer as well as the journal editors provided useful and constructive comments.

## References

- Alexandri M, Papanikolaou D, Nomikou P, Ballas D (2001) Geological structure of the Myrtoon basin (Aegean Sea) based on swath bathymetry. *Rapp Comm Int Mer Medit* 36
- Bell KLC, Carey S, Nomikou P, Sigurdsson H, Sakellariou D (2013) Submarine evidence of a debris avalanche deposit on the eastern slope of Santorini volcano, Greece. *Tectonophysics* 597(598):147–160
- Canals M, Lastras G, Urgeles R, Casamor J, Mienert J, Cattaneo A, De Batist M, Haflidason H, Imbo Y, Laberg JS, Locat J, Long D, Longva O, Masson DG, Sultan N, Trincardi F, Bryn P (2004) Slope failure dynamics and impacts from seafloor and shallow sub-seafloor geophysical data: case studies from the COSTA project. *Marine Geology* 213:9–72
- Carey SN, Schneider J (2011) Volcaniclastic processes and deposits in the deep-sea. In: Hüneke H, Mulder T (eds) *Deep sea sediments*, vol 63, *Developments in Sedimentology*. Elsevier, Amsterdam, pp 457–515
- Cassidy M, Trofimovs J, Palmer MR, Talling PJ, Watt SFL, Moreton SG, Taylor RN (2013) Timing and emplacement dynamics of newly recognised mass flow deposits at 8–12 ka offshore Soufrière Hills volcano, Montserrat: how submarine stratigraphy can complement subaerial eruption histories. *Journal of Volcanology and Geothermal Research* 253:1–14
- Deplus C, Le Friant A, Boudon G, Komorowski JC, Villeman B, Harford C (2001) Submarine evidence for large-scale debris avalanches in the Lesser Antilles Arc. *Earth and Planetary Science Letters* 192:145–157
- Dufresne A, Davies TR (2009) Longitudinal ridges in mass movement deposits. *Geomorphology* 105:171–181
- Fontán Bouzas A, Alcántara-Carrió J, Montoya Montes I, Barranco Ojeda A, Albarracín S, Díaz R, de Rada J, Rey Salgado J (2013) Distribution and thickness of sedimentary facies in the coastal dune, beach and nearshore sedimentary system at Maspalomas, Canary Islands. *Geo-Marine Letters* 33(2/3):117–127. doi:10.1007/s00367-012-0313-z
- Glicken H (1991) Sedimentary architecture of large volcanic-debris avalanches. In: Fisher RV, Smith GA (eds), *Sedimentation in volcanic settings*. SEPM Spec Publ 45:99–106
- Katsouras G, Gogou A, Bouloubassi I, Emeis KC, Triantaphyllou M, Roussakis G, Lykousis V (2010) Organic carbon distribution and isotopic composition in three records from the eastern Mediterranean Sea during the Holocene. *Organic Geochemistry* 41:935–939
- Krastel S, Schmincke H-U, Jacobs CL, Rihm R, Alibes B, Le Bas TP (2001) Submarine landslides around the Canary Islands. *Journal of Geophysical Research* 106:3977–3997
- Le Pichon X, Angelier J (1979) The Hellenic arc and trench system: a key to the neotectonic evolution of the Eastern Mediterranean area. *Tectonophysics* 60:1–42
- Lipman PW, Normark WR, Moore JG, Wilson JB, Gutmacher CE (1988) The giant submarine Alike debris slide, Mauna Loa, Hawaii. *Journal of Geophysical Research* 93:4279–4299
- Løseth H, Gading M, Wensaas L (2009) Hydrocarbon leakage interpreted on seismic data. *Mar Petrol Geol* 26(7):1304–1319
- Lykousis V (2009) Sea-level changes and shelf break prograding sequences during the last 400 ka in the Aegean margins: subsidence rates and palaeogeographic implications. *Continental Shelf Research* 29:2037–2044
- Marini L, Principe C, Chiodini G, Cioni R, Fytikas M, Marinelli G (1993) Hydrothermal eruptions of Nisyros (Dodecanese, Greece). Past events and present hazard. *Journal of Volcanology and Geothermal Research* 56:71–94
- McKenzie DP (1970) Plate tectonics of the Mediterranean region. *Nature* 226:239–243
- Mitchell NC, Quartau R, Madeira J (2012) Assessing landslide movements in volcanic islands using near-shore marine geophysical data: south Pico Island, Azores. *Bulletin of Volcanology* 74(2):483–496
- Nomikou P, Papanikolaou D (2011) Extension of active fault zones on Nisyros volcano across the Yali-Nisyros Channel based on onshore and offshore data. *Marine Geophysical Research* 32(1/2):181–192. doi:10.1007/s11001-011-9119-z
- Nomikou P, Tibaldi A, Pasquare F, Papanikolaou D (2009) Submarine morphological analysis based on multibeam data of a huge collapse at the SE flank of Nisyros volcano. *Ext Abstr Poster Int Conf Seafloor Mapping for Geohazard Assessment*, 11–13 May, Ischia. *Rendiconti Online Società Geologica Italiana* 7:177–179
- Nomikou P, Papanikolaou D, Alexandri M, Sakellariou D, Rousakis G (2013) Submarine volcanoes along the Aegean volcanic arc. *Tectonophysics* 597(598):123–146
- Papanikolaou D (1993) Geotectonic evolution of the Aegean. *Bull Geol Soc Greece* 28(1):33–48
- Papanikolaou D, Lekkas E, Sakellariou D (1991) Volcanic stratigraphy and evolution of the Nisyros volcano. *Bull Geol Soc Greece* 25:405–419
- Shaller PJ (1991) Analysis and implications of large Martian and terrestrial landslides. PhD thesis, CalTech, Pasadena
- Siebert L (1984) Large volcanic debris avalanches: characteristics of source areas, deposits and associated eruptions. *Journal of Volcanology and Geothermal Research* 22:163–197
- Tibaldi A, Pasquare FA, Papanikolaou D, Nomikou P (2008) Discovery of a huge sector collapse at the Nisyros volcano, Greece, by on-land and offshore geological-structural data. *Journal of Volcanology and Geothermal Research* 177:485–499
- Tomlinson EL, Kinvig HS, Smith VC, Blundy JD, Gottsmann J, Müller W, Menzies MA (2012) The Upper and Lower Nisyros Pumices: revisions to the Mediterranean tephrostratigraphic record based on micron-beam glass geochemistry. *Journal of Volcanology and Geothermal Research* 243–244:69–80
- Triantaphyllou MV, Ziveri P, Gogou A, Marino G, Lykousis V, Bouloubassi I, Emeis KC, Kouli K, Dimiza M, Rosell-Mele A, Papanikolaou M, Katsouras G, Nunez N (2009a) Late Glacial-Holocene climate variability at the southeastern margin of the Aegean Sea. *Marine Geology* 266:182–197
- Triantaphyllou MV, Antonarakou A, Kouli K, Dimiza M, Kontakiotis G, Papanikolaou MD, Ziveri P, Mortyn PG, Lianou V, Lykousis V, Dermitzakis MD (2009b) Late Glacial-Holocene ecostratigraphy of the south-eastern Aegean Sea, based on plankton and pollen assemblages. *Geo-Marine Letters* 29(4):249–267. doi:10.1007/s00367-009-0139-5
- Voight B, Glicken H, Janda RJ, Douglass PM (1981) Catastrophic rockslide avalanche of May 18. In: Lipman PW, Mullineaux DR (eds), *The 1980 eruptions of Mount St. Helens*. Washington, DC, US Geol Surv Prof Paper 1250:347–378
- Voight B, Janda RJ, Glicken H, Douglass PM (1983) Nature and mechanics of the Mount St. Helens rockslide-avalanche of 18 May 1980. *Geotechnique* 33:243–273